#### REVIEW



# Review of Computational Approaches to Optimization Problems in Inhomogeneous Rods and Plates

Weitao Chen<sup>1</sup> · Chiu-Yen Kao<sup>2</sup>

Received: 17 August 2022 / Revised: 5 December 2022 / Accepted: 6 December 2022 © Shanghai University 2023

#### Abstract

In this paper, we review computational approaches to optimization problems of inhomogeneous rods and plates. We consider both the optimization of eigenvalues and the localization of eigenfunctions. These problems are motivated by physical problems including the determination of the extremum of the fundamental vibration frequency and the localization of the vibration displacement. We demonstrate how an iterative rearrangement approach and a gradient descent approach with projection can successfully solve these optimization problems under different boundary conditions with different densities given.

**Keywords** Inhomogeneous rods and plates  $\cdot$  Bi-Laplacian  $\cdot$  Optimization of eigenvalues  $\cdot$  Localization of eigenfunctions  $\cdot$  Rearrangement

Mathematics Subject Classification 35P05 · 35P15 · 35Q93 · 65K10 · 65N25

#### 1 Introduction

This article is dedicated to our esteemed collaborator and friend: Ching-Shan Chou. Words can never express enough how much we miss her. About ten years ago, we worked on optimization problems involving inhomogeneous rods and plates together at The Ohio State University. Even though we are in different places now, we hope that this review article acts like a time machine and brings us all back to the old time when we all lived, laughed, and loved.

Weitao Chen and Chiu-Yen Kao have contributed equally to this work.

Chiu-Yen Kao ckao@cmc.edu

Weitao Chen weitaoc@ucr.edu

Published online: 28 March 2023

Department of Mathematical Sciences, Claremont McKenna College, 850 Columbia Ave, Claremont, CA 91711, USA



Department of Mathematics, University of California at Riverside, 900 University Ave, Riverside, CA 92521, USA

The study of vibrating rods and plates have attracted a lot of attention since the eighteenth century. Euler (April 15, 1707 – September 18, 1783) used calculus of variation technique to determine the critical axial compressive load with which a cylindrical column has lateral deflection [19]. Later Lagrange (January 25, 1736 – April 10, 1813) formulated the problem to maximize the critical load of a rod of variable cross-sectional area with given length and volume, but he did not succeed in getting the correct solution [25]. Chladni (November 30, 1756 – April 3, 1827) discovered different nodal lines pattern of a vibrating plate when he spread sand on the plate and stroke it with a violin bow [11]. This experiment became publicly known at that time. The king Napoleon was also fascinated by the beauty of patterns and decided to give a prize for the underlying mathematical theory. The prize was awarded to Germain (April 1, 1776 – June 27, 1831) in 1816 [34] who provided the first satisfactory solution. Later, the theory was completed by Kirchhoff (March 12, 1824 – October 17, 1887) who found that Chladni figures on a square plate correspond to nodal lines of eigenfunctions of the bi-Laplacian operator with free boundary conditions [18, 22].

Nowadays, one can easily generate Chladni figures at home with a medal plate attached to a mechanical wave driver which provides designated frequency and amplitude. Spread sand on a medal plate and tune the frequency until it resonates. The sand will move toward the nodal lines which correspond to the locations with the least amount of vibration. See Fig. 1 with three different vibrating frequencies.

Let  $\Omega$  be a bounded open set in  $\mathbb{R}^d$  with the Lipschitz boundary  $\partial\Omega$ . For ease of exposition, the dimension d is chosen to be one or two here, even though the study can be easily extended to higher dimensions. The inhomogeneity of the rods and plates (i.e., d=1 and d=2, respectively) is characterized by a non-constant mass density function  $\rho$ . The governing equation of a vibrating rod or a square plate with uniform thickness is

$$\rho(\mathbf{x})\frac{\partial^2 \phi(t, \mathbf{x})}{\partial t^2} + D\Delta^2 \phi(t, \mathbf{x}) = 0, \quad \mathbf{x} \in \Omega,$$
 (1)

where D is the flexural rigidity and  $\Delta^2 = \Delta \Delta$  is the bi-Laplacian operator in the spatial variables. Assuming the natural vibration solution to be periodic, i.e.,

$$\phi = u(\mathbf{x})e^{ikt},\tag{2}$$

where u is the transverse displacement which only depends on the position coordinates and k is the circular frequency. Substituting (2) into (1) leads to the eigenvalue problem

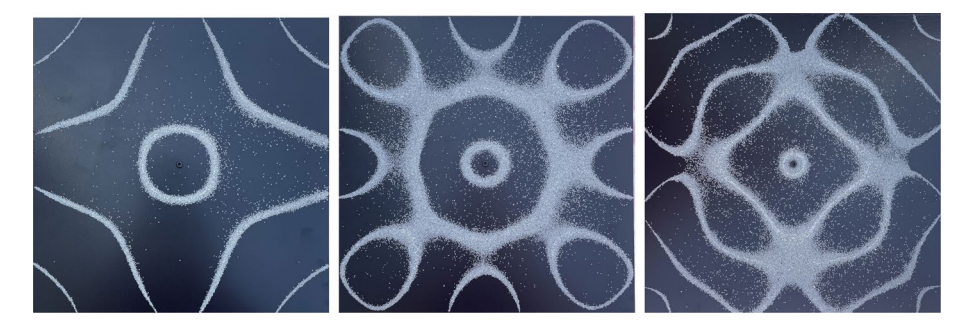


Fig. 1 The sand patterns of a plate which vibrates at three different frequencies (photos taken by authors)



$$\Delta^2 u(\mathbf{x}) = \lambda \rho(\mathbf{x}) u(\mathbf{x}),\tag{3}$$

where  $\lambda = k^2/D$ .

Here, we consider two types of boundary conditions: the clamped boundary that both the displacement and its slope are zero, i.e.,

$$\mathcal{B}_{c}: \left\{ u(t, \mathbf{x}) = u_{n}(t, \mathbf{x}) = 0, \mathbf{x} \in \partial \Omega \right\}, \tag{4}$$

or the hinged boundary

$$\mathcal{B}_{h}^{\kappa}: \left\{ u(t, \mathbf{x}) = \Delta u(t, \mathbf{x}) - (1 - \nu)(\kappa u_{n}) = 0, \mathbf{x} \in \partial \Omega \right\}, \tag{5}$$

where  $\nu$  is the Poisson's ratio satisfying  $-1 \le \nu \le 0.5$ ,  $u_n = \hat{n} \cdot \nabla u$ ,  $\hat{n}$  is the outward unit normal vector, and  $\kappa$  is the curvature at the boundary [32]. On the straight boundary of  $\Omega \subset \mathbb{R}^2$ , i.e.,  $\kappa = 0$ , the hinged boundary can be reduced to

$$\mathcal{B}_{\mathbf{b}}^{0} \colon \{ u(t, \mathbf{x}) = \Delta u(t, \mathbf{x}) = 0, \mathbf{x} \in \partial \Omega \}. \tag{6}$$

We will focus on problems on an interval or a square plate, so only (4) or (6) will be used. For other shapes of plates and their corresponding boundary conditions, see [17, 27, 35] for governing equations and solutions.

The spectrum of (3) with aforementioned boundary conditions is discrete and the eigenvalues can be enumerated, counting multiplicity, in an increasing order

$$0 < \lambda_1 \leqslant \lambda_2 \leqslant \cdots \leqslant \lambda_i \leqslant \cdots \to \infty$$
.

In this paper, we review approaches to design the mass density to optimize objective functions that depend on bi-Laplacian eigenvalues and eigenfunctions. Assume that the density function is in the class of the admissible density with a fixed total mass:

$$\mathcal{A}_{\alpha,\beta,\gamma}(\varOmega) = \left\{ \rho(\mathbf{x}) \in L^{\infty}(\varOmega); \alpha \leqslant \rho(\mathbf{x}) \leqslant \beta \text{ a.e. in } \varOmega, \ \int_{\varOmega} \rho(\mathbf{x}) \mathrm{d}\mathbf{x} = \gamma \right\},$$

where  $\alpha$ ,  $\beta$ , and  $\gamma$  are nonzero given constants with  $0 < \alpha < \beta$  and  $\alpha |\Omega| \le \gamma \le \beta |\Omega|$ . We consider the extremum problem

$$\min_{\rho(\mathbf{x}) \in \mathcal{A}_{\alpha,\beta,\gamma}} \mathcal{J}(\lambda(\rho(\mathbf{x})), u(\rho(\mathbf{x}))), \tag{7}$$

where  $\mathcal{J}(\cdot)$  represents a function of a specific eigenvalue and its corresponding eigenfunction. Other possible admissible sets will be discussed later. In particular, we will focus on two different problems: one is to optimize eigenvalues [9, 30] while the other is to localize eigenfunctions [10, 16]. These two kinds of problems are motivated by physical problems. One is to determine the minimum and maximum of the fundamental vibration frequency while the other is to localize the vibration displacement.

For the optimization of eigenvalues, the density to minimize (or maximize) the first eigenvalue,  $\lambda_1$ , is found to be the same for a clamped rod and a hinged rod [4–6, 33]. For a higher eigenvalue,  $\lambda_j$  ( $j \ge 2$ ), only the extremal density for a hinged rod is known analytically. In [20, p.183], the determination of the optimal density distribution for the clamped rod problem with  $j \ge 2$  was listed as an open question. Later, motivated by numerical results, it was proved that the optimal density that minimizes  $\lambda_j$  ( $j \ge 2$ ) for a clamped rod must be distinct from the one for a hinged rod [9]. The existence and properties of optimal densities for plates were



considered recently in [1, 13–15]. In spite of these nice theoretical results, the optimal density distribution can only be precisely identified when  $\Omega$  is a ball [13, 30]. For the localization of eigenfunctions for rods and plates [3, 10, 24, 28], theoretical results are quite scattered. To find solutions to these inhomogeneous optimization problems, numerical approaches become necessary.

This paper is organized as follows. In Sect. 2, the variational characterization of eigenvalues is reviewed and the variations of eigenvalues and eigenfunctions with respect to the mass density are derived. In Sect. 3, we introduce the classical theoretical results of optimization of *j*-th bi-Laplacian eigenvalue problems and an iterative rearrangement algorithm to minimize the first eigenvalue. In Sect. 4, we discuss a gradient descent approach with projection to localize the chosen eigenfunctions. In Sect. 5, the discrete approximation based on finite difference methods is discussed in detail. The numerical implementation of aforementioned approaches is provided. In Sect. 6, we demonstrate that the numerical approaches successfully solve both optimization problems over rods and plates. A brief conclusion of our paper with a discussion is given in Sect. 7.

## 2 Variational Formulas

In this section, several variational formulas involve eigenvalues and eigenfunctions will be discussed. Consider the space  $\mathbb{H}(\Omega) = H_0^2(\Omega)$  for the clamped boundary (4) or  $\mathbb{H}(\Omega) = H_0^1(\Omega) \cap H^2(\Omega)$  for the hinged boundary (6). Multiplying (3) by  $\psi \in \mathbb{H}(\Omega)$  and integrating by parts, one obtains the corresponding variational formulation of (3): find  $\lambda \in \mathbb{R}$  and  $u \in \mathbb{H}(\Omega)$ ,  $u \neq 0$  such that

$$\int_{\Omega} \Delta u(\mathbf{x}) \Delta \psi(\mathbf{x}) d\mathbf{x} = \lambda \int_{\Omega} \rho(\mathbf{x}) u(\mathbf{x}) \psi(\mathbf{x}) d\mathbf{x}$$
 (8)

for all  $\psi \in \mathbb{H}(\Omega)$ .

Denote  $(\lambda_j, u_j)$  as the *j*-th eigenpair. The variational formulations of the eigenvalues [1] are

$$\lambda_1(\rho) = \min_{\psi \in \mathbb{H}(\Omega), \psi \neq 0} \frac{\int_{\Omega} (\Delta \psi)^2 d\mathbf{x}}{\int_{\Omega} \rho \psi^2 d\mathbf{x}},\tag{9}$$

and

$$\lambda_{j}(\rho) = \min_{\substack{E_{j} \subset \mathbb{H}(\Omega), \\ \text{subspace of dim } j}} \max_{\psi \in E_{j}, \psi \neq 0} \frac{\int_{\Omega} (\Delta \psi)^{2} d\mathbf{x}}{\int_{\Omega} \rho \psi^{2} d\mathbf{x}}$$
(10)

for higher eigenmodes  $j \ge 2$ . To solve the optimization problem (7), we first derive the dependence of the eigenvalues and eigenfunctions on the variation of the mass density. By the min-max principle, it is clear that  $\lambda_j$  is a locally Lipschitz continuous function of  $\rho$  [26]. Since eigenfunctions are defined up to a constant, we normalize the eigenfunction by the condition

$$\int_{\Omega} \rho(\mathbf{x}) u^2(\mathbf{x}) d\mathbf{x} = 1. \tag{11}$$



**Proposition 1** Let  $(\lambda, u)$  be a simple bi-Laplacian eigenpair, satisfying (3) with the boundary condition (4) or (6), normalized so that  $\int_{\Omega} \rho u^2 d\mathbf{x} = 1$ . Consider a perturbation  $\rho \mapsto \rho + \tau \eta$ . Then, (a) the functional  $\rho \mapsto \lambda(\rho)$  is Frechét differentiable with derivative

$$\dot{\lambda} = \partial_{\rho} \lambda(\rho)(\eta) := \partial_{\rho} \lambda(\rho + \tau \eta)_{\tau=0} = -\lambda \int_{\Omega} u^{2}(\mathbf{x}) \eta(\mathbf{x}) d\mathbf{x}, \tag{12}$$

and (b) the derivative of u satisfies

$$\Delta^2 \dot{u} - \lambda \rho \dot{u} - 2\lambda \rho u \int_{\Omega} \rho u \dot{u} d\mathbf{x} = \lambda \eta u \tag{13}$$

with the corresponding clamped or hinged boundary condition.

**Proof** (a) We take a derivative of the formula  $\lambda = \int_{\Omega} (\Delta u)^2 d\mathbf{x}$  and use Green's identity to obtain

$$\begin{split} \dot{\lambda} &= 2 \int_{\Omega} \Delta \dot{u} \Delta u \mathrm{d}\mathbf{x} \\ &= 2 \int_{\partial \Omega} \dot{u}_n \Delta u \mathrm{d}S - 2 \int_{\Omega} \nabla \dot{u} \cdot \nabla (\Delta u) \mathrm{d}\mathbf{x} \\ &= 2 \int_{\partial \Omega} \dot{u}_n \Delta u \mathrm{d}S - 2 \int_{\partial \Omega} \dot{u} (\Delta u)_n \mathrm{d}S + 2 \int_{\Omega} \dot{u} \Delta^2 u \mathrm{d}\mathbf{x} \\ &= 2 \lambda \int_{\Omega} \rho u \dot{u} \mathrm{d}\mathbf{x}, \end{split}$$

where  $u_n = \hat{n} \cdot \nabla u$  and  $\hat{n}$  is the outward unit normal vector. From the normalization condition,  $\int_O \rho u^2 d\mathbf{x} = 1$ , we obtain

$$\int_{\Omega} \dot{\rho} u^2 d\mathbf{x} = -2 \int_{\Omega} \rho u \dot{u} d\mathbf{x},$$

which gives the desired result.

(b) Taking a derivative of (3) leads to

$$\Delta^2 \dot{u} = \dot{\lambda} \rho u + \lambda \dot{\rho} u + \lambda \rho \dot{u}.$$

By using the equality obtained in (a), we have

$$\Delta^2 \dot{u} - \lambda \rho \dot{u} - 2\lambda \rho u \int_{\Omega} \rho u \dot{u} d\mathbf{x} = \lambda \eta u.$$

The derivative of the boundary condition (4) or (6) leads to the corresponding clamped or hinged boundary condition for  $\dot{u}$ .



# 3 Optimization of j-th Eigenvalue

One of the classical spectrum problems is to determine the range of eigenvalues, e.g., what is the range of the first eigenvalue of (3) with the clamped or hinged boundary when  $\rho \in \mathcal{A}_{\alpha,\beta,\gamma}$ ? This corresponds to the determination of the minimal and maximal fundamental frequencies, i.e.,  $\mathcal{J}(\lambda, u) := \lambda_1$ , of a rod or a plate with a fixed total mass.

In one dimension, the optimal densities  $\rho(\mathbf{x})$  corresponding to the extremal  $\lambda_j$  are proved to be of bang-bang type for both kinds of boundary conditions [4–6, 33]. This means that  $\rho$  takes the value  $\alpha$  or  $\beta$ . Thus, we consider the admissible mass density in the set

$$\bar{\mathcal{A}}_{\alpha,\beta,\gamma}(\Omega) = \{ \rho(\mathbf{x}) = \beta \chi_D + \alpha \chi_{\Omega \setminus D} \}, \tag{14}$$

where  $D \subset \Omega$  and  $\beta |D| + \alpha(|\Omega| - |D|) = \gamma$ . This implies that  $|D| = \frac{\gamma - \alpha |\Omega|}{\beta - \alpha}$ . The eigenvalue problem of an inhomogeneous clamped rod is

$$\begin{cases} u^{(4)}(x) = \lambda \rho(x)u(x), \text{ in } [-L, L], \\ u(-L) = u'(-L) = u(L) = u'(L) = 0, \end{cases}$$

while the one of a hinged (simply supported) rod is

$$\begin{cases} u^{(4)}(x) = \lambda \rho(x)u(x), & \text{in } [-L, L], \\ u(-L) = u''(-L) = u(L) = u''(L) = 0. \end{cases}$$

Then, the unique minimizer  $\check{\rho}_1(x)$  (maximizer  $\hat{\rho}_1(x)$ ) of both clamped and hinged extremal eigenvalue problems  $\min_{\rho} \lambda(\rho)$  ( $\max_{\rho} \lambda(\rho)$ ) in the class of  $\mathcal{A}_{\alpha,\beta,\gamma}$  is

$$\check{\rho}_1(x) = \begin{cases} \alpha, & x \in (-L, -\delta), \\ \beta, & x \in (-\delta, \delta), \\ \alpha, & x \in (\delta, L), \end{cases} \begin{pmatrix} \hat{\rho}_1(x) = \begin{cases} \beta, & x \in (-L, -\delta), \\ \alpha, & x \in (-\delta, \delta), \\ \beta, & x \in (\delta, L), \end{cases},$$

where

$$\delta = \frac{\gamma - 2\alpha L}{2\beta - 2\alpha} = \frac{\gamma - 2\beta L}{2\alpha - 2\beta}.$$
 (15)

This optimal distribution is the same as the one for the Dirichlet Laplace eigenvalue problem

$$\begin{cases} -u''(x) = \lambda \rho(x)u(x), \text{ in } [-L, L], \\ u(-L) = u(L) = 0, \end{cases}$$

which was discovered by Krein [23]. He also found that optimal distributions for general higher eigenmodes  $\lambda_j$  ( $j \ge 2$ ) of the Dirichlet Laplace eigenvalue problem are 2L/j-periodic and are defined on each interval

$$\left(-L+\frac{2nL}{j},-L+\frac{2(n+1)L}{j}\right),\quad n=0,\cdots,j-1$$

by

$$\rho_{j}(x) = \check{\rho}_{1}(jx - (2n+1-k)L), \quad \rho_{j}(x) = \hat{\rho}_{1}(jx - (2n+1-k)L). \tag{16}$$



Banks [5] found that the optimal density distributions for  $\lambda_j$  for a hinged rod are exactly the same as (16). However, the optimal density for a clamped rod is unknown. Later, numerical results that were obtained via a rearrangement algorithm proposed in [9] demonstrate that the optimal density configuration for the clamped rod must be distinct from the one for the hinged rod. Furthermore, this was verified analytically via an asymptotic approach for j = 2 [9].

Two-dimensional problems were considered recently in [1, 13–15]. In [1, 14, 15], the authors studied the minimization and maximization of the first eigenvalue for several given materials of fixed volumes. The existence of minimizers in the family of all measurable functions which are rearrangements of a given function was proved for both clamped and hinged boundary conditions; however, the existence of maximizers can be proved only for domain  $\Omega$  such that the operator is positive preserving, i.e.,  $u \ge 0$  if  $\Delta^2 u = f$  in  $\Omega$  with clamped boundary conditions for any given  $f \ge 0$ . Assuming that every level set of eigenfunction has measure zero, the extremum occurs when the density function is a monotone increasing (decreasing) function of the square of the eigenfunction corresponding to the eigenvalue which is to be minimized (maximized) [1, 14, 15]. This implies that the material with the higher (lower) density must be located at places where the magnitude of the eigenfunction is larger (smaller). In [13], the optimal density  $\rho \in \mathcal{A}_{\alpha,\beta,\gamma}$  to minimize the first eigenvalue is shown to be of bang-bang type, i.e., the plate can be made only out of two materials, whose densities are given by the constants  $\alpha$  and  $\beta$ .

# 3.1 Iterative Rearrangement Algorithm for Minimization of First Eigenvalues

Here we discuss two important properties that will be used to generate an iterative rearrangement algorithm.

**Proposition 2** Assume  $(\lambda_a, u_a)$  and  $(\lambda_b, u_b)$  are first eigenpairs satisfying (3) with the boundary condition (4) or (6) corresponding to mass densities  $\rho_a$  and  $\rho_b$ , respectively. If

$$\int_{\Omega} \rho_a u_b^2 d\mathbf{x} > \int_{\Omega} \rho_b u_b^2 d\mathbf{x},\tag{17}$$

then the first eigenvalues satisfy

$$\lambda_a < \lambda_b. \tag{18}$$

**Proof** First, normalize the eigenfunctions such that  $\int_{\Omega} (\Delta u_a)^2 d\mathbf{x} = \int_{\Omega} (\Delta u_b)^2 d\mathbf{x} = 1$ . By using the variational characterization of the first eigenvalue (9),

$$\begin{split} \lambda_{a} &= \inf_{\psi \in \mathbb{H}(\Omega), \psi \neq 0} \frac{\int_{\Omega} (\Delta \psi)^{2} \mathrm{d}\mathbf{x}}{\int_{\Omega} \rho_{a} \psi^{2} \mathrm{d}\mathbf{x}} = \frac{1}{\int_{\Omega} \rho_{a} u_{a}^{2} \mathrm{d}\mathbf{x}} \\ &< \frac{1}{\int_{\Omega} \rho_{a} u_{b}^{2} \mathrm{d}\mathbf{x}} \\ &< \frac{1}{\int_{\Omega} \rho_{b} u_{b}^{2} \mathrm{d}\mathbf{x}} \text{(inequality (17))}. \end{split}$$

**Definition 1** Two Lebesgue measurable density functions,  $\rho_a : \Omega \subset \mathbb{R}^d \to \mathbb{R}$  and  $\rho_b : \Omega \subset \mathbb{R}^d \to \mathbb{R}$ , are said to be density rearrangements of each other if



$$|\{\mathbf{x} \in \Omega : \rho_a(\mathbf{x}) \geqslant c\}| = |\{\mathbf{x} \in \Omega : \rho_b(\mathbf{x}) \geqslant c\}|, \qquad \forall c \in \mathbb{R}.$$
 (19)

**Proposition 3** Let  $\mathcal{P}$  be the set of all possible density rearrangements of a fixed mass density function  $\rho_b \in \mathcal{A}_{\alpha,\beta,\gamma}$  of bang-bang type. Denote  $(\lambda_b,u_b)$  as the first eigenpair of (3) with the mass density  $\rho_b$  and the boundary condition (4) or (6). Then, the maximization problem

$$\sup_{\rho \in \mathcal{P}} \int_{\Omega} \rho u_b^2 d\mathbf{x} \tag{20}$$

is uniquely solved by  $\check{\rho} = \beta \chi_D + \alpha \chi_{\Omega \setminus D}$  such that

$$D = \{ \mathbf{x} \in \Omega : u_b^2 \geqslant t \},\tag{21}$$

where  $t = \sup_{s} \left\{ \left| \left\{ \mathbf{x} \in \Omega : u_b^2 \geqslant s \right\} \right| \geqslant \frac{\gamma - \alpha |\Omega|}{\beta - \alpha} \right\}.$ 

**Proof** See [30, Theorem 2.1 and Lemma 5.4] for a proof.

Based on Propositions 2 and 3, one can generate a sequence of mass density functions  $\{\rho^{(i)}\}$  such that their corresponding first eigenvalues  $\{\lambda_1^{(i)}\}$  form a monotone decreasing sequence. Since the first eigenvalue is bounded below, this sequence converges and it was observed numerically that it converges to the minimizer  $\check{\rho}$ . At the *i*-th iteration, we first solve (3) with the density function  $\rho^{(i)}$  to obtain the first eigenpair  $(\lambda_1^{(i)}, u_1^{(i)})$ . By applying Propositions 3 to  $u_1^{(i)}$ , we can find a new density function such that the high density region is a sup-level set of  $(u_1^{(i)})^2$  and

$$\int_{\Omega} \rho^{(i+1)}(u_1^{(i)})^2 d\mathbf{x} > \int_{\Omega} \rho^{(i)}(u_1^{(i)})^2 d\mathbf{x}.$$

Proposition 2 guarantees that the eigenvalue  $\lambda^{(i+1)}$  corresponding to  $\rho^{(i+1)}$  satisfies  $\lambda^{(i+1)} < \lambda^{(i)}$ .

# 4 Localization of Eigenfunctions

The optimal localization of eigenfunctions in an inhomogeneous medium has raised in the design of mechanical vibration and optical devices [2, 16]. Here we consider the following function which is the one proposed in [10, 16] to measure the degree of location by the moment:

$$\mathcal{J}(\rho) := \frac{1}{2} \int_{\Omega} w \rho u_j(\rho)^2 d\mathbf{x}, \tag{22}$$

where  $u_j$  is the normalized j-th eigenfunction, and w is the weight function which penalizes the nonlocalization, e.g.,  $w = (x - x_0)^2$ . The density function is assumed to be bounded

$$\mathcal{A}_{\alpha,\beta}(\Omega) = \{ \rho(x) \in L^{\infty}(\Omega); \alpha \leqslant \rho(x) \leqslant \beta \text{ a.e. in } \Omega \}.$$

The goal is to localize the eigenfunction  $u_j$  that corresponds to the vibration displacement at the given location  $x_0$ . One can also design the localization of an eigenfunction along an arbitrary curved boundary by changing the weight function. See [10] for examples.



As it is unknown whether the optimal density is of bang-bang type, we use a gradient descent approach with projection. Here we discuss the derivative of the objective function first.

**Proposition 4** Let  $(\lambda_j, u_j)$  be the simple j-th bi-Laplacian eigenpair, satisfying (3) with the boundary condition (4) or (6), normalized so that  $\int_{\Omega} \rho u_j^2 d\mathbf{x} = 1$ . Consider a perturbation  $\rho \mapsto \rho + \tau \eta$ . Then, the derivative of (22) is

$$\dot{\mathcal{J}} = \int_{\Omega} \eta \left( \frac{1}{2} w u_j^2 + \lambda_j u_j v_j \right) d\mathbf{x},\tag{23}$$

where  $v_i$  satisfies the adjoint equation

$$\Delta^2 v - \lambda \rho v - 2\lambda \rho u_j \int_{\Omega} \rho u_j v d\mathbf{x} = \rho w_i u_j$$
 (24)

with the corresponding clamped or hinged boundary condition.

**Proof** Taking derivative of the energy function (22) and plugging the formula (12) lead to

$$\dot{\mathcal{J}}(\rho) = \frac{1}{2} \int_{\Omega} w \eta u_j^2 d\mathbf{x} + \int_{\Omega} w \rho u_j \dot{u}_j \mathbf{x} d\mathbf{x}.$$

Multiplying (4) by  $\dot{u}_i$  and integrating over the domain  $\Omega$  lead to

$$\int_{\Omega} w \rho u_j \dot{u}_j d\mathbf{x} = \int_{\Omega} \Delta^2 v_j \dot{u}_j d\mathbf{x} - \lambda_j \int_{\Omega} \rho v \dot{u}_j d\mathbf{x} - 2\lambda_j \int_{\Omega} \rho u \dot{u}_j d\mathbf{x} \int_{\Omega} \rho u_j v_j d\mathbf{x}.$$

Multiplying (1) by v and integrating over the domain  $\Omega$  give

$$\int_{\Omega} \Delta^{2} \dot{u}_{j} v_{j} d\mathbf{x} - \lambda_{j} \int_{\Omega} \rho \dot{u}_{j} v_{j} d\mathbf{x} - 2\lambda_{j} \int_{\Omega} \rho u_{j} v_{j} d\mathbf{x} \int_{\Omega} \rho u_{j} \dot{u}_{j} d\mathbf{x} = \lambda_{j} \int_{\Omega} \eta u_{j} v_{j} d\mathbf{x}.$$
 (25)

One can then integrate by parts to obtain

$$\int_{\Omega} w \rho u_j \dot{u}_j d\mathbf{x} = \lambda_j \int_{\Omega} \eta u_j v_j d\mathbf{x}.$$
 (26)

Thus,

$$\dot{\mathcal{J}}(\rho) = \int_{\Omega} \eta \left( \frac{1}{2} w u_j^2 + \lambda_j u_j v_j \right) d\mathbf{x}.$$

The gradient direction is

$$g := \frac{1}{2}wu_j^2 + \lambda_j u_j v_j, \tag{27}$$

and the normalized descent gradient direction is  $-g/\|g\|$ . After each gradient descent step, we project the density function back to the admissible set  $\mathcal{A}_{\alpha,\beta}(\Omega)$ .



# 5 Numerical Approaches

#### 5.1 The Finite Difference Forward Solver

Even though there are many different numerical approaches, e.g., finite element approaches [8, 12, 29, 31] and spectral approaches [7], to solve (3), we review the easiest approach based on the finite difference methods [9].

In one dimension, without loss of generality, we choose  $\Omega = [-1, 1]$  and a uniform mesh  $\mathbf{x_g} := \{x_i\}_{0 \le i \le N} = \{-1 + ih\}_{0 \le i \le N}$  where h is the mesh size and N = 2/h. The discretized eigenfunction is denoted by  $\mathbf{U}$  in the form of a column vector  $(U_0, \dots, U_N)^T$  which approximates  $(u(x_0), \dots, u(x_N))^T$  numerically. The fourth order derivative at  $x_i$  is approximated by the central difference formula

$$U_{i}^{''''} \approx \frac{U_{i-2} - 4U_{i-1} + 6U_{i} - 4U_{i+1} + U_{i+2}}{L^{4}}$$

for  $i = 2, \dots, N-2$  which yields a second-order accuracy. To approximate the derivatives at  $x_1$  and  $x_{N-1}$ , values at ghost points  $x_{-1} = -1 - h$  and  $x_{N+1} = 1 + h$  are needed and can be derived by the given boundary conditions. If clamped boundary conditions are imposed, that is,

$$u(-1) = u(1) = u'(-1) = u'(1) = 0,$$

then we choose  $U_0 = U_N = 0$  at two end points and  $U_{-1} = U_1$  and  $U_{N+1} = U_{N-1}$  at two ghost points. Thus,

$$U_1^{\prime\prime\prime\prime} \approx \frac{7U_1 - 4U_2 + U_3}{h^4},$$

and

$$U_{N-1}^{""} \approx \frac{U_{N-3} - 4U_{N-2} + 7U_{N-1}}{h^4}.$$

The hinged boundary conditions

$$u(-1) = u(1) = u''(-1) = u''(1) = 0$$

lead to  $U_0 = U_N = 0$  at the boundaries,  $U_{-1} = 2U_0 - U_1$  and  $U_{N+1} = 2U_N - U_{N-1}$  at two ghost points. Thus,

$$U_1^{""} \approx \frac{5U_1 - 4U_2 + U_3}{h^4},$$

and

$$U_{N-1}^{''''} \approx \frac{U_{N-3} - 4U_{N-2} + 5U_{N-1}}{h^4}.$$

Consequently, the matrix representing the bi-Laplacian operator on [-1,1] is formed by assigning the coefficients in the approximation formula of  $U_i^{'''}$  to the *i*-th row.

In a two-dimensional rectangle  $\Omega = [-a,a] \times [-b,\dot{b}]$ , define a uniform mesh  $\mathbf{x}_g = \{(x_{1i},x_{2j})\} := \{-a+ih_1,-b+jh_2\}$  where  $h_1$  and  $h_2$  are mesh sizes in  $x_1$ - and



 $x_2$ -directions, respectively. For simplicity, we assume that  $h_1 = h_2 = h$ . Let  $(U_{i,j})_{0 \le i \le N, 0 \le j \le M}$  be the matrix of the discretized eigenfunction where  $Nh_1 = 2a$  and  $Mh_2 = 2b$ . The second-order central difference scheme involving 13-point stencils is used to approximate the bi-Laplacian operator

$$\Delta^2 U_{i,j} \approx \frac{1}{h^4} \left[ \begin{array}{cccc} & + U_{i,j+2} \\ & + 2U_{i-1,j+1} & - 8U_{i,j+1} & + 2U_{i+1,j+1} \\ + U_{i-2,j} & - 8U_{i-1,j} & + 20U_{i,j} & - 8U_{i+1,j} & U_{i+2,j} \\ & + 2U_{i-1,j-1} & - 8U_{i,j-1} & + 2U_{i+1,j-1} \\ & & + U_{i,j-2} \end{array} \right]$$

for  $2 \le i \le N-2$  and  $2 \le j \le M-2$ . With clamped boundary conditions, the bi-Laplacian operator along i=1 is approximated by

$$\Delta^2 U_{1,j} \approx \frac{1}{h^4} \left[ \begin{array}{ccc} +U_{1,j+2} & & \\ -8U_{1,j+1} & +2U_{2,j+1} & \\ +21U_{1,j} & -8U_{2,j} & U_{3,j} \\ -8U_{1,j-1} & +2U_{2,j-1} & \\ +U_{1,j-2} & \end{array} \right], \quad 2 \leqslant j \leqslant M-2,$$

and

$$\Delta^2 U_{1,1} \approx \frac{1}{h^4} \begin{bmatrix} +U_{1,3} \\ -8U_{1,2} & +2U_{2,2} \\ +22U_{1,1} & -8U_{2,1} & U_{3,1} \end{bmatrix}.$$

The approximating formulas along i = N - 1, j = 1, or j = M - 1 can be derived similarly. All points at the boundaries are taken as zero,  $U_{0,j} = U_{N,j} = U_{i,0} = U_{i,M} = 0$ . For the hinged boundary conditions, the discretization is almost the same, except the approximations for points near the boundaries (i = 1 or N - 1, j = 1 or M - 1). For example,

$$\Delta^2 U_{1,j} \approx \frac{1}{h^4} \begin{bmatrix} +U_{1,j+2} \\ -8U_{1,j+1} & +2U_{2,j+1} \\ +19U_{1,j} & -8U_{2,j} & U_{3,j} \\ -8U_{1,j-1} & +2U_{2,j-1} \\ +U_{1,j-2} \end{bmatrix}, \quad 2 \leq j \leq M-2,$$

and

$$\Delta^2 U_{1,1} \approx \frac{1}{h^4} \begin{bmatrix} +U_{1,3} \\ -8U_{1,2} & +2U_{2,2} \\ +18U_{1,1} & -8U_{2,1} & U_{3,1} \end{bmatrix}.$$

The discretization along the other sides can be obtained similarly. Each stencil approximating  $\Delta^2 U_{i,j}$  is assigned into a row to form the matrix of the discrete bi-Laplacian operator. Therefore, the size of the matrix to approximate the bi-Laplacian operator on a rectangle is  $(N-1)(M-1) \times (N-1)(M-1)$ .

In summary, at the discrete level, (3) with the specified boundary is approximated by



$$AU = BU\Lambda$$
.

where  $\mathbb{A}$ ,  $\mathbb{B}$ ,  $\mathbb{U}$ , and  $\Lambda$  are discrete approximations of the bi-Laplacian operator with specified boundary condition, the mass density function  $\rho$ , the eigenfunction u, and the eigenvalue  $\lambda$ , respectively. Note that  $\mathbb{B}$  and  $\Lambda$  are diagonal matrices.

## 5.2 Optimization Solver

## 5.2.1 Iterative Rearrangement Algorithm for Minimization of Eigenvalues

As described in the aforementioned section, for any given mass density function  $\rho(\mathbf{x})$ , we form the discrete bi-Laplacian operator  $\mathbb{A}$  and the matrix  $\mathbb{B}$  with its diagonal element  $\rho(\mathbf{x_g})$  where  $\mathbf{x_g}$  are gridpoints of a mesh. The Arnoldi iteration is used to solve the forward eigenvalue problem  $\mathbb{A}\mathbf{U} = \mathbb{B}\mathbf{U}\Lambda$  to obtain approximated eigenvalues which are diagonal elements of  $\Lambda$  and corresponding approximated eigenfunctions which are columns of  $\mathbf{U}$ .

At the *i*-th iteration, denote  $\rho^{(i)}$  as the mass density function and  $(\lambda_1^{(i)}, \mathbf{U}_1^{(i)})$  as the corresponding first eigenpair. To look for the new density  $\rho^{(i+1)}$ , we determine the set  $D^{(i+1)}$  such that (21) is satisfied. This implies that the high density region is a sup-level set of  $(u_1^{(i)})^2$ . On a uniform mesh, it is extremely easy to implement this numerically. One can simply first estimate the number of grid that takes the high density by computing  $\mathcal{N} := \left\lfloor \frac{1}{\Delta x} \frac{\gamma - \alpha |\Omega|}{\beta - \alpha} \right\rfloor$  where  $\Delta \mathbf{x}$  is the grid size, i.e.,  $\Delta \mathbf{x} = \Delta x$  in one dimension and  $\Delta \mathbf{x} = \Delta x_1 \Delta x_2$  in two dimensions. Then, sort  $(\mathbf{U}_1^{(i)})^2$  in the descending order and assign the high density  $\beta$  to the points corresponding to first  $\mathcal{N}$  largest of  $(\mathbf{U}_1^{(i)})^2$ .

Compared with the gradient descent approach, this rearrangement of the density approach is far more efficient. Usually, the rearrangement algorithm converges in a few iterations unlike the gradient descent approach which usually takes hundreds of iterations [21].

**Remark 1** The algorithm described here for the first eigenvalue can be applied to minimize simple  $\lambda_j$  for  $j \ge 2$ . However, it is possible that the j-th eigenvalue becomes multiple, that is, it collides with its neighboring eigenvalues. When this happens, multiple eigenfunctions need to be considered while updating the density function: instead of the order of  $(\mathbf{U}_j^{(i)})^2$ , we should arrange  $\rho_j$  in the order of the convex combination  $\sum_{s=0}^c \alpha_s (\mathbf{U}_{(j-s)}^{(i)})^2$  where the real numbers  $\alpha_s$ 's satisfy  $\alpha_s \ge 0$  and  $\sum_{s=0}^c \alpha_s = 1$  if  $\lambda_{j-c}, \cdots, \lambda_j$  collide. One can perform an optimization algorithm to find the optimal  $\alpha_s$ 's which give the largest integral (20) or simply choose a combination such that the integral increases at each iteration.

We summarize the minimization algorithm in Algorithm 1.



# **Algorithm 1** A rearrangement algorithm for minimization of $\lambda_i$

```
Require Input: given \alpha, \beta, and \gamma, choose an initial \rho^{(0)} \in \bar{\mathcal{A}}_{\alpha,\beta,\gamma}(\Omega).
   Set i = 0.
   Solve the bi-Laplacian eigenvalue problem (3) by the finite difference method
   discussed in Sect. 5.1
   while \rho^{(i)} is not optimal do
        if the eigenvalue \lambda_j is colliding with its neighbors \lambda_{j-c}, \dots, \lambda_{j-1} then
              sort the linear combination \eta := \sum_{s=0}^{c} \alpha_s(\mathbf{U}_{i-s}^{(i)})^2 with \sum_{s=0}^{c} \alpha_s = 1
   in a descending order
         else
              sort \eta := (\mathbf{U}_{i}^{(i)})^{2} in a descending order
   Compute \mathcal{N} = \left\lfloor \frac{1}{\Delta \mathbf{x}} \frac{\gamma - \alpha |\Omega|}{\beta - \alpha} \right\rfloor. Assign the high density \beta to the points corresponding to first \mathcal{N} largest of \eta
        if \|\rho^{(i)} - \rho^{(i+1)}\| = 0 then
              Stop
        else
              solve the bi-Laplacian eigenvalue problem (3) with \rho^{(i+1)}
              set i := i + 1
         end if
   end while
```

#### 5.2.2 Gradient Descent Method

We discuss a similar approach to the one in [10, 16] to minimize the energy (22). Here we directly work with the eigenfunction u instead of defining a new variable  $\rho^{\frac{1}{2}}u$  that are used in [10, 16]. At the i-th iteration, assume  $\rho^{(i)}$  is the mass density. We first compute the eigenpair  $(\lambda_i, u_i)$ ,  $1 \le k \le n$ . Next, the adjoint equation (4) is discretized as

$$\mathbb{A}\mathbf{V}_{i} - \lambda_{i} \mathbb{B}\mathbf{V}_{i} - 2\lambda_{i} \mathbb{B}\mathbf{U}_{i} (\mathbb{B}\mathbf{U})_{i}^{\mathsf{T}} \mathbf{V}_{i} \Delta \mathbf{x} = \mathbb{B}\mathbf{W}\mathbf{U}_{i}, \tag{28}$$

where  $\mathbb{A}$  is a discrete bi-Laplacian operator,  $\mathbb{B}$  is a diagonal matrix with its diagonal element  $\rho(\mathbf{x}_g)$ ,  $\mathbf{V}$  is the adjoint variable,  $(\lambda_j, \mathbf{U}_j)$  is the j-th eigenpair,  $\mathbf{W}$  is a discrete weight matrix with its diagonal element  $w(\mathbf{x}_g)$ , and  $\Delta \mathbf{x}$  is the grid size. We solve for  $\mathbf{V}_j$  for each  $\mathbf{U}_j$ . The gradient direction can be computed via (27) which leads to

$$g := \left\{ \frac{1}{2} \mathbf{W} \mathbf{U}_j. * \mathbf{U}_j + \lambda_j \mathbf{U}_j. * \mathbf{V}_j \right\}. \tag{29}$$

Here the dot multiplication .\* means the element-wise multiplication for two vectors which results in a vector. We summarize the gradient descent approach with projection to the admissible set to localize eigenfunctions in Algorithm 2.



Algorithm 2 A gradient descent algorithm for localization of the j-th eigenfunction

```
Require Input: given \alpha, \beta, x_0, j, and the stepsize \tau_o > 0, choose an initial \rho^{(0)} \in \mathcal{A}_{\alpha,\beta}(\Omega).

Set i = 0.

(i) Solve the bi-Laplacian eigenvalue problem (3) by the finite difference method discussed in Sect. 5.1.

(ii) Solve the adjoint equation (28).

(iii) Compute the normalized descent gradient direction -g/\|g\| with g defined in (29).

(iv) Compute \rho = \rho^{(i)} - \tau g/\|g\| with \tau = \tau_0 and \mathcal{J}(\rho).

while \mathcal{J}(\rho) > \mathcal{J}(\rho^{(i)}) and \tau > 10^{-15} do

Set \tau = \tau/2 and compute \rho = \rho^{(i)} - \tau g/\|g\| and \mathcal{J}(\rho).

end while \rho = \min (\max(\rho, \alpha), \beta)

Set \rho^{i+1} = \rho and i = i+1 and check for convergence. If no convergence and \tau is not too small, continue with Step (i).
```

### 6 Numerical Tests

In this section, we demonstrate that the iterative rearrangement method and the gradient descent method with projection can successfully solve optimization problems including the minimization of eigenvalues and the localization of eigenfunctions for rods and plates with hinged or clamped boundary conditions.

# 6.1 Minimization of Eigenvalues for Rods

We consider the minimization of eigenvalues on an interval [-L, L] with L = 1 for a rod consisting of two different materials, i.e.,  $\rho = \alpha$  or  $\rho = \beta$ , described in Sect. 3. The iterative rearrangement algorithm is applied to achieve the optimal density distribution of a bang-bang type. For simplicity, we let  $\gamma = (\alpha + \beta)L$  be the fixed total mass. The analytical formula (15) for the hinged rod implies that  $\delta = L/2$  which is independent of material densities  $\alpha$  and  $\beta$ . This is true for any other choices of  $\gamma$  once the area of regions with different densities is fixed. We have also observed this behavior numerically. For a hinged rod, the minimizers of  $\lambda_i$  for  $i=1,\cdots,6$  are identical for  $\beta=8$  (Fig. 2) and 16 (Fig. 3). For a clamped boundary rod, since the analytical formulas of minimizers are not available, numerical study of the optimal density distributions is performed. In particular, it has been discovered that the optimal density distributions for a clamped rod are not periodic as the optimal ones for a hinged rod [9]. Here, the outmost subregions with the higher density have larger areas than the inner subregions. See the optimal density distributions for  $\beta = 8$ and 16 in Figs. 2 and 3, respectively. More specifically, we measure the length of each subregion in minimizers and the results are shown in Tables 1 and 2. For all computed eigenmodes, the lengths of subregions in the minimizers are almost identical, suggesting the optimal density distributions with clamped boundary conditions are also independent of densities.



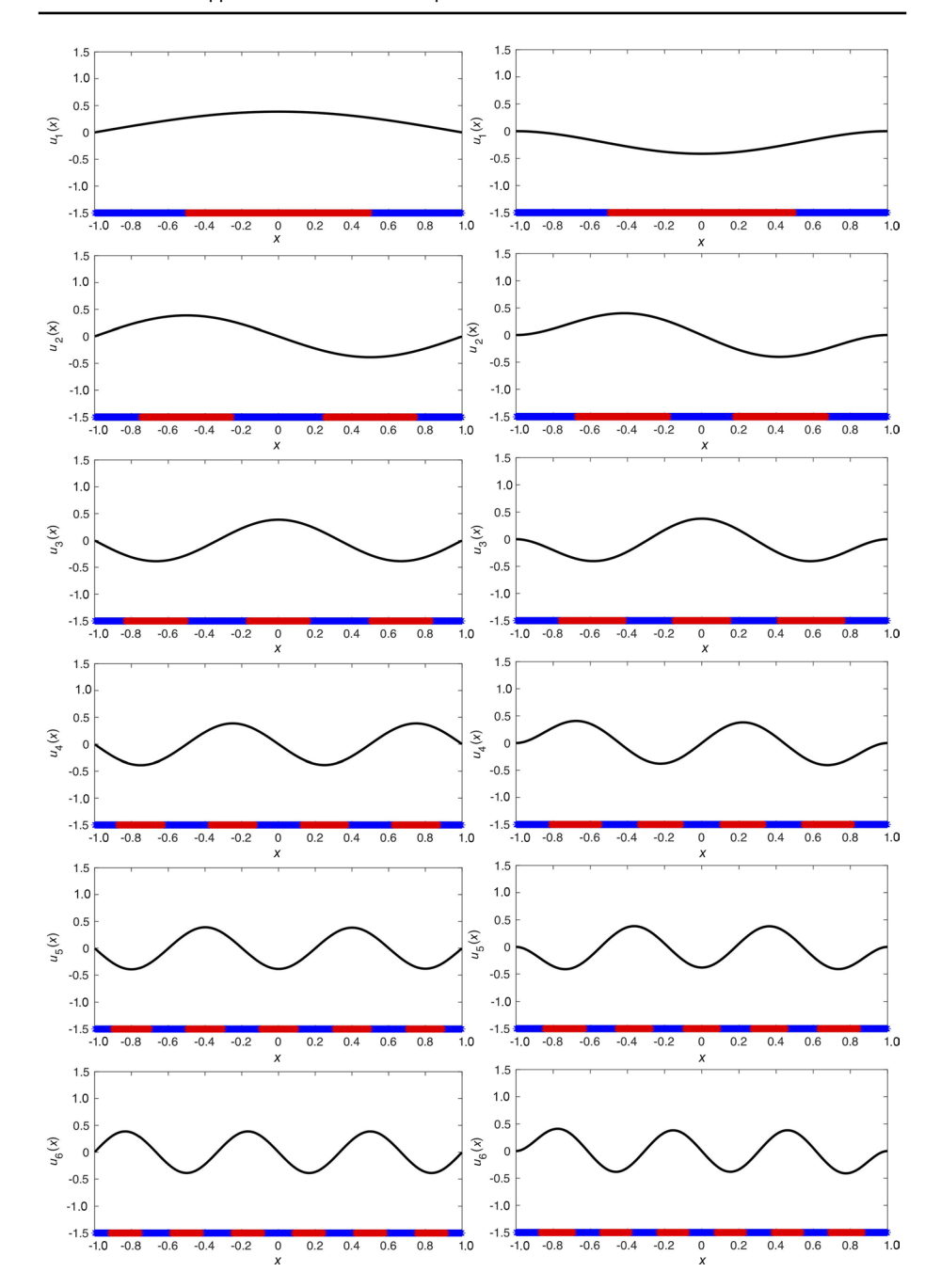


**Fig. 2** The optimal density distributions (red  $(\rho(x) = \beta)$  and blue  $(\rho(x) = \alpha = 1)$ ) and their corresponding eigenfunctions for the minimization of the first six eigenvalues with hinged (left) or clamped (right) boundary conditions for  $\beta = 8$ 



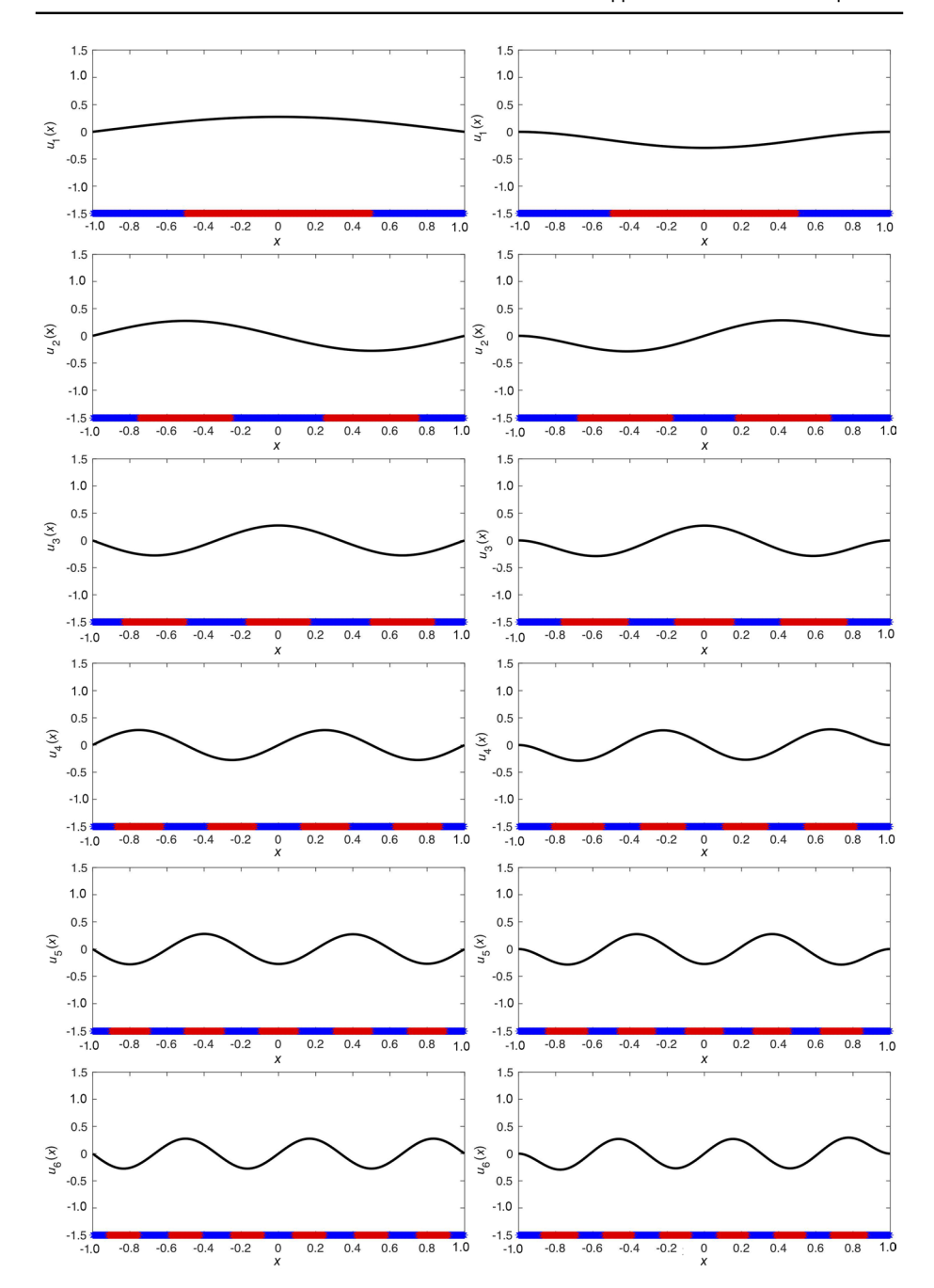


**Fig. 3** The optimal density distributions and their corresponding eigenfunctions for the minimization of the first six eigenvalues with hinged (left) or clamped (right) boundary conditions for  $\beta = 16$ 



**Table 1** Lengths of subregions in the minimizers with clamped boundary conditions for  $\beta = 8$ 

	Lengths of subregions
$\lambda_1$	[0.50 1.00 0.50] <i>L</i>
$\lambda_2$	[0.33 0.50 0.35 0.50 0.33]L
$\lambda_3$	$[0.24\ 0.35\ 0.27\ 0.30\ 0.27\ 0.35\ 0.24]L$
$\lambda_4$	$[0.19\ 0.27\ 0.21\ 0.23\ 0.21\ 0.23\ 0.21\ 0.27\ 0.19]L$
$\lambda_5$	$[0.15\ 0.21\ 0.17\ 0.19\ 0.18\ 0.19\ 0.17\ 0.19\ 0.17\ 0.21\ 0.15]L$
$\lambda_6$	$[0.13\ 0.18\ 0.15\ 0.16\ 0.15\ 0.16\ 0.15\ 0.16\ 0.15\ 0.16\ 0.15\ 0.16\ 0.15\ 0.18\ 0.13]L$

**Table 2** Lengths of subregions in the minimizers with clamped boundary conditions for  $\beta = 16$ 

	Lengths of subregions
$\lambda_1$	[0.50 1.00 0.50]L
$\lambda_2$	$[0.33\ 0.50\ 0.35\ 0.50\ 0.33]L$
$\lambda_3$	$[0.24\ 0.35\ 0.26\ 0.31\ 0.26\ 0.35\ 0.24]L$
$\lambda_4$	$[0.19\ 0.27\ 0.21\ 0.23\ 0.21\ 0.23\ 0.21\ 0.27\ 0.19]L$
$\lambda_5$	$[0.15\ 0.21\ 0.17\ 0.19\ 0.17\ 0.19\ 0.17\ 0.19\ 0.17\ 0.21\ 0.15]L$
$\lambda_6$	$[0.13\ 0.19\ 0.15\ 0.16\ 0.15\ 0.16\ 0.15\ 0.16\ 0.15\ 0.16\ 0.15\ 0.19\ 0.13]L$

# 6.2 Minimization of Eigenvalues for Plates

For a square plate, the optimal density distributions to minimize the first five eigenvalues are shown in Figs. 4 and 5 for  $\beta = 8$  and  $\beta = 16$ , respectively. As uncovered in [9], optimal density distributions with hinged and clamped boundary conditions followed similar patterns with different locations for high density subregions. We further explore different values for the higher density and measure areas of subregions at the higher density. For  $\beta = 8$  and 16, the optimal density distributions for the corresponding eigenmode are not distinguishable from each other. Areas of subregions at the higher density are also more or less the same, suggesting the optimal density distributions are independent of density values when fixing areas of subregions with the lower and higher densities in two dimensions. This is consistent with the one dimensional case.

## 6.3 Localization of a Single Eigenfunction in One Dimension

Next, we study the localization of some specific eigenfunction at some specific location. In this example, we consider localizing the 6th eigenfunction at a single point. Notice that, with the homogeneous density, the 6th eigenfunction has a small magnitude at 0.15 and a large magnitude at 0.25 [9]. Therefore, we try to localize the 6th eigenfunction at a single point for those two scenarios and obtain the optimal density distributions, respectively. The results are shown in Fig. 6. For the case with  $x_0 = 0.15$ , since the eigenfunction does not have a big vibration displacement with the homogeneous density, in the optimizer two nearest amplitude peaks are brought to the chosen location to achieve a higher displacement there. For the case with  $x_0 = 0.25$ , the eigenfunction has

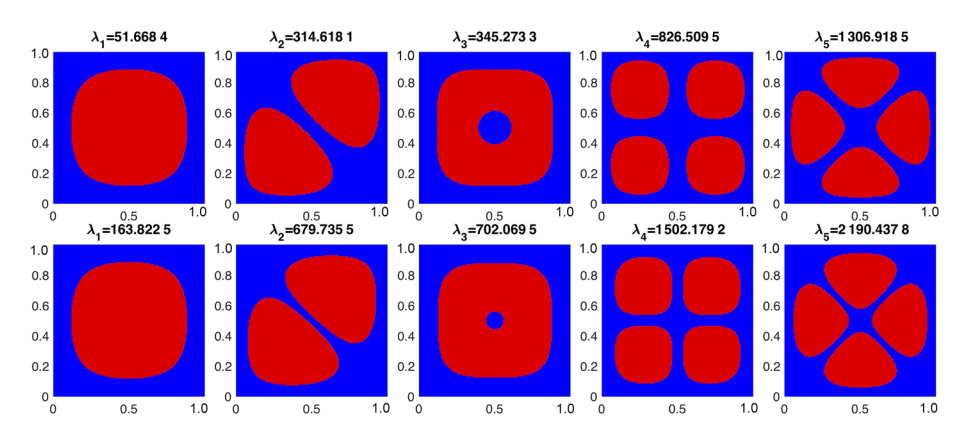


**Fig. 4** The optimal density distributions and their corresponding eigenfunctions for the minimization of the first five eigenvalues with hinged (the first row) or clamped (the second row) boundary conditions for  $\beta = 8$ 

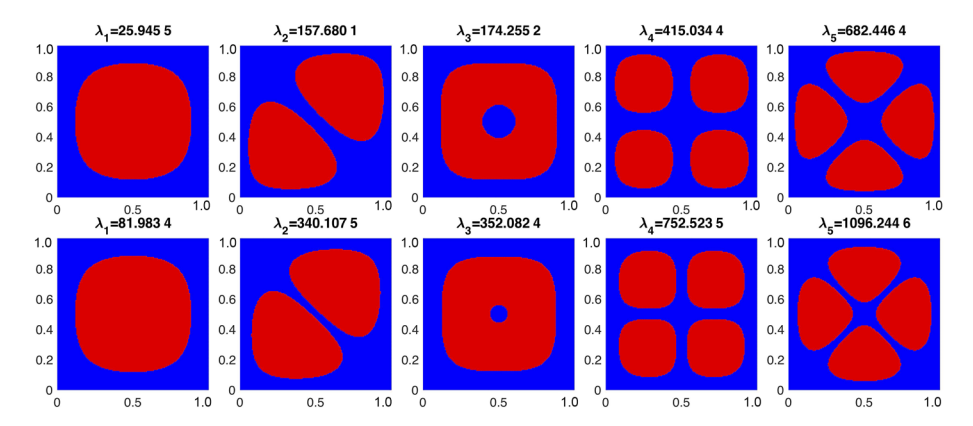


Fig. 5 The optimal density distributions and their corresponding eigenfunctions for the minimization of the first five eigenvalues with hinged (the first row) or clamped (the second row) boundary conditions for  $\beta = 16$ 

a big vibration displacement originally when the density is homogeneous and this peak is kept in the optimizer. In addition, one neighboring vibration peak with the homogeneous density is also amplified in the optimizer to achieve a larger displacement at the chosen location. We also test the optimization problems with different values of the higher density,  $\beta = 8$  or 16. The optimized density profiles are quite similar to each other with only minor changes (See Fig. 6).

## 6.4 Localization of a Single Eigenfunction in Two Dimensions

We also study the localization problems in two dimensions. In particular, we try to localize the 11th eigenfunction at (0, 0) with different boundary conditions and different values of the higher density. The optimal density distributions are shown in Fig. 7.



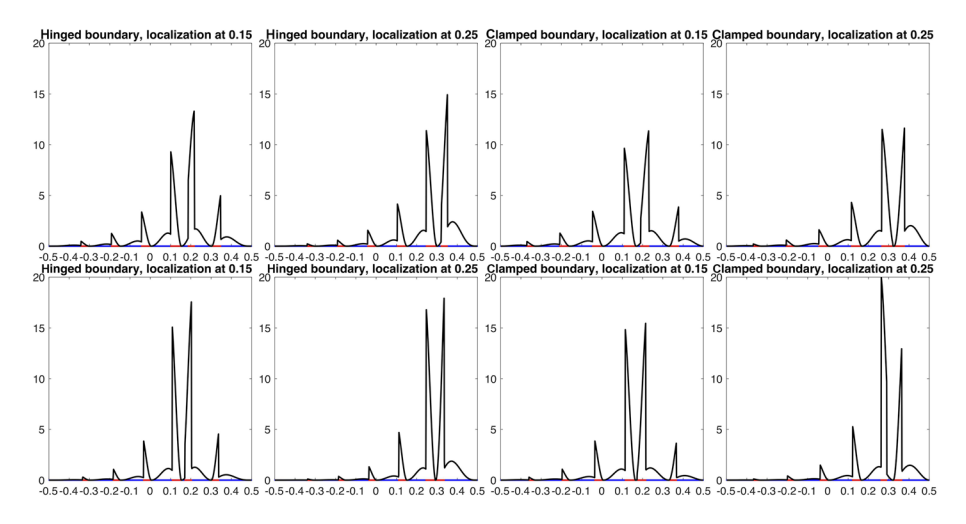
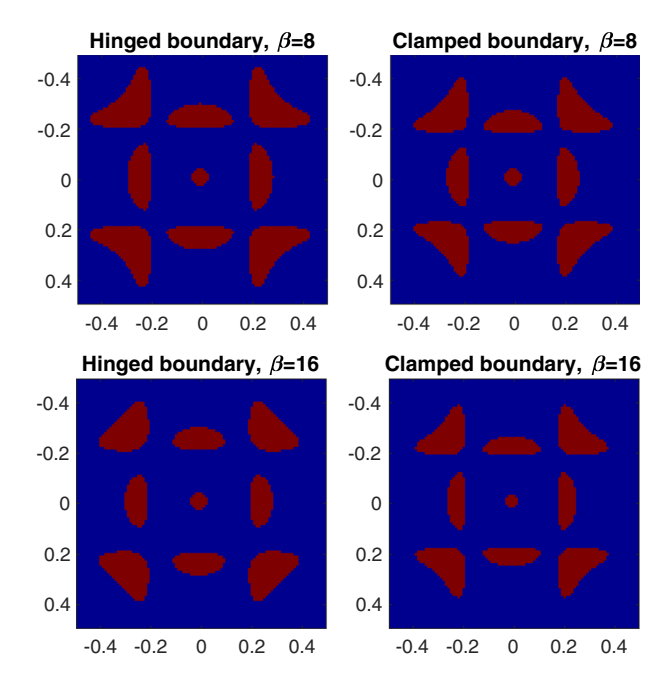


Fig. 6 The optimal density distributions and  $\rho u^2$  (curves in black) for localizing the 6th eigenfunction at 0.15 or 0.25 with hinged or clamped boundary conditions and for  $\beta = 8$  (top) or 16 (bottom), respectively

In general, hinged boundary and clamped boundary conditions give rise to similar optimal distribution patterns. Subregions with the higher density are located more tightly and closer to the center with the clamped boundary conditions. By increasing the higher density, subregions at the higher density are shrunk with locations unchanged.

**Fig. 7** The optimal density distributions for localizing the 11th eigenfunction at (0, 0) with hinged or clamped boundary conditions for  $\beta = 8$  and 16, respectively





## 7 Conclusion and Discussion

In this paper, we review briefly the history of the optimization problems of inhomogeneous rods and plates, and computational methods to optimize eigenvalues or localize eigenfunctions with hinged or clamped boundary conditions. Variational formulas are derived for both types of optimization problems with different boundary conditions. Numerical discretization of the forward problem is described in detail. To optimize eigenvalues, the iterative rearrangement algorithm is applied for efficiency. To localize eigenfunctions, a gradient descent method is applied. We test those two numerical approaches on different optimization problems with different boundary conditions. Both are shown to be numerically effective and accurate. The numerical results are consistent with theoretical formulas or previously published ones. The effect of the boundary conditions is quite consistent with what have been reported. In both cases, optimal density distributions with clamped boundary conditions have subregions with the higher density more concentrated near the center of the entire domain, compared with those obtained under hinged boundary conditions. Moreover, we test those methods on problems with different values of the high density  $\beta$ . For minimization of eigenvalues, it is observed that the optimal density distributions are independent of densities once the areas corresponding to different densities are fixed, no matter what boundary conditions are imposed. For localization of eigenfunctions, optimal density distributions have some small changes on the size of subregions with different densities. The framework discussed in this paper can be easily applied to more complicated objective functions depending on eigenvalues and eigenfunctions. We hope to investigate more and report numerical results in the near future.

**Author Contributions** The authors contributed equally to this work.

**Funding** Weitao Chen is partially supported by the DMS-1853701. Chiu-Yen Kao's work is supported in part by the DMS-2208373.

**Code Availability** Codes are available upon request.

# **Compliance with Ethical Standards**

**Conflict of Interest** The authors declare no conflict of interest.

### References

- Anedda, C., Cuccu, F., Porru, G.: Minimization of the first eigenvalue in problems involving the bi-Laplacian. Revista de Mat. Teor. Apl. 16(1), 127–136 (2009)
- Arnold, D.N., David, G., Filoche, M., Jerison, D., Mayboroda, S.: Localization of eigenfunctions via an effective potential. Comm. Partial Differential Equations 44(11), 1186–1216 (2019)
- 3. Bakharev, F., Matveenko, S.: Localization of eigenfunctions in a narrow Kirchhoff plate. Russ. J. Math. Phys. **28**(2), 156–178 (2021)
- 4. Banks, D.O.: Bounds for the eigenvalues of some vibrating systems. Pac. J. Math. 10(2), 439-474 (1960)
- Banks, D.O.: Bounds for the eigenvalues of nonhomogeneous hinged vibrating rods. J. Math. Mech. 16, 949– 966 (1967)
- Beesack, P.R.: Isoperimetric inequalities for the nonhomogeneous clamped rod and plate. J. Math. Mech. 8, 471–482 (1959)
- Bjørstad, P.E., Tjøstheim, B.P.: High precision solutions of two fourth order eigenvalue problems. Computing 63(2), 97–107 (1999)
- Brenner, S.C., Monk, P., Sun, J.: C<sup>0</sup> interior penalty Galerkin method for biharmonic eigenvalue problems. In: Spectral and High Order Methods for Partial Differential Equations ICOSAHOM 2014, pp. 3–15. Springer, Switzerland (2015)



- Chen, W., Chou, C.-S., Kao, C.-Y.: Minimizing eigenvalues for inhomogeneous rods and plates. J. Sci. Comput. 69(3), 983–1013 (2016)
- Chen, W., Diest, K., Kao, C.-Y., Marthaler, D.E., Sweatlock, L.A., Osher, S.: Gradient based optimization methods for metamaterial design. In: Numerical Methods for Metamaterial Design, pp. 175–204. Springer, Dordrecht (2013)
- 11. Chladni, E.F.F.: Die Akustik. Breitkopf & Härtel, Leipzig (1802)
- Ciarlet, P.G., Raviart, P.-A.: A mixed finite element method for the biharmonic equation. In: Mathematical Aspects of Finite Elements in Partial Differential Equations, pp. 125–145. Academic Press, New York (1974)
- Colasuonno, F., Vecchi, E.: Symmetry in the composite plate problem. Commun. Contemp. Math. 21(02), 1850019 (2019)
- Cuccu, F., Emamizadeh, B., Porru, G.: Optimization of the first eigenvalue in problems involving the bi-Laplacian. Proceed. Am. Math. Soc. 137(5), 1677–1687 (2009)
- Cuccu, F., Porru, G.: Maximization of the first eigenvalue in problems involving the bi-Laplacian. Nonlinear Anal. Theory Methods Appl. 71(12), 800–809 (2009)
- Dobson, D.C., Santosa, F.: Optimal localization of eigenfunctions in an inhomogeneous medium. SIAM J. Appl. Math. 64(3), 762–774 (2004)
- Elishakoff, I.: Eigenvalues of Inhomogeneous Structure. Unusual Closed-Form Solutions. CRC Press, Boca Raton (2004)
- Gander, M.J., Kwok, F.: Chladni figures and the Tacoma bridge: motivating PDE eigenvalue problems via vibrating plates. SIAM Rev. 54(3), 573–596 (2012)
- 19. Gautschi, W.: Leonhard Euler: his life, the man, and his works. SIAM Rev. 50(1), 3–33 (2008)
- Henrot, A.: Extremum Problems for Eigenvalues of Elliptic Operators. Springer, Basel-Boston-Berlin (2006)
- Kao, C.-Y., Su, S.: Efficient rearrangement algorithms for shape optimization on elliptic eigenvalue problems. J. Sci. Comput. 54(2/3), 492–512 (2013)
- Kirchhoff, G.: Über das gleichgewicht und die bewegung einer elastischen scheibe. J. Die Reine Angew. Math. (Crelles Journal) 1850(40), 51–88 (1850)
- Krein, M.G.: On Certain Problems on the Maximum and Minimum of Characteristic Values and on the Lyapunov Zones of Stability. American Mathematical Society translations. American Mathematical Society, Boston (1955)
- Kropinski, M., Lindsay, A., Ward, M.: Asymptotic analysis of localized solutions to some linear and nonlinear biharmonic eigenvalue problems. Stud. Appl. Math. 126(4), 347–408 (2011)
- 25. Lagrange, J.-L.: Sur la figure des colonnes. Miscellanea Taurinensia 5, 123–166 (1770)
- Lamberti, P.D., Provenzano, L.: A maximum principle in spectral optimization problems for elliptic operators subject to mass density perturbations. arXiv:1205.5624 (2012)
- Leissa, A.W.: Vibration of Plates. Scientific and Technical Information Division, National Aeronautics and Space Adminstration, Washington, D.C. (1969)
- Lindsay, A.E., Quaife, B., Wendelberger, L.: A boundary integral equation method for mode elimination and vibration confinement in thin plates with clamped points. Adv. Comput. Math. 44(4), 1249–1273 (2018)
- Meng, J., Mei, L.: The optimal order convergence for the lowest order mixed finite element method of the biharmonic eigenvalue problem. J. Comput. Appl. Math. 402, 113783 (2022)
- Mohammadi, S., Bahrami, F.: Extremal principal eigenvalue of the bi-Laplacian operator. Appl. Math. Model. 40(3), 2291–2300 (2016)
- 31. Monk, P.: A mixed finite element method for the biharmonic equation. SIAM J. Numer. Anal. **24**(4), 737–749 (1987)
- 32. Nazarov, S.A., Sweers, G.: A hinged plate equation and iterated Dirichlet Laplace operator on domains with concave corners. J. Differential Equations 233(1), 151–180 (2007)
- Schwarz, B.: Some results on the frequencies of nonhomogeneous rods. J. Math. Anal. Appl. 5(2), 169– 175 (1962)
- 34. Stöckmann, H.-J.: Chladni meets Napoleon. Eur. Phys. J. Spec. Top. 145(1), 15–23 (2007)
- Wang, C.Y., Wang, C.: Structural Vibration: Exact Solutions for Strings, Membranes, Beams, and Plates. CRC Press, Boca Raton (2013)

Springer Nature or its licensor (e.g., a society or other partner) holds exclusive rights to this article under a publishing agreement with the author(s) or other rightsholder(s); author self-archiving of the accepted manuscript version of this article is solely governed by the terms of such publishing agreement and applicable law.

